RSC Advances

PAPER

View Article Online
View Journal | View Issue

Cite this: *RSC Adv.*, 2019, **9**, 30207

Improved hydrogen production in the single-chamber microbial electrolysis cell with inhibition of methanogenesis under alkaline conditions

Wanjun Cui, Guangli Liu, Cuiping Zeng, Yaobin Lu,* Haiping Luo and Renduo Zhang

Received 17th July 2019
Accepted 11th September 2019

DOI: 10.1039/c9ra05483a

rsc.li/rsc-advances

The aim of this study was to investigate hydrogen production enhanced by methanogenesis inhibition in the single-chamber microbial electrolysis cell (MEC) under alkaline conditions. With 50 mM bicarbonate buffer and 1 g L^{-1} acetate, the MEC was tested at pH = 8.5, 9.5, 10.5, and 11.2, respectively, within 124 d operation. Effective methanogenesis inhibition in the MEC increased with pH from 8.5 to 11.2. At pH 11.2, Methanobacteriaceae reached the lowest absolute quantity (*i.e.*, biomass and *mcrA* gene copy number of methanogens) within the microbial community in the cathodic biofilm among the pH values. Under the alkaline conditions, a hydrogen percentage of 85–90% and a methane percentage < 15% were achieved within 25 cycles (50 d) of operation. The maximum current density in the MEC reached 83.7 ± 1.5 A m^{-3} with the average electrical recovery of 171 ± 18% and overall energy recovery of 72 ± 3%. The excellent performance of the MEC at pH = 11.2 was attributed to the low abundance of methanogens within the cathodic biofilm (2.23 ± 0.46 copy per cm^2), low cathodic biomass (0.12 ± 0.01 mg protein per g), and low anode potential (−0.228 mV *vs.* saturated calomel electrode). Results from this study should be valuable to expand applications of the MEC with methanogenesis inhibition in alkaline wastewater treatment.

1. Introduction

With high energy density and clean combustion product, hydrogen (H_2) has been considered as an ideal alternative energy source to fossil fuel.[1,2] Compared with the conventional H_2 production processes, such as chemical refinery, water electrolysis, and dark-fermentation, the microbial electrolysis cell (MEC) emerges as a promising and attractive technology with advantages of mild operation conditions, efficient biomass conversion to biohydrogen gas, and high coulombic efficiency (CE).[2,3] Under an applied voltage of 0.30 V (*vs.* standard H_2 electrode), electrons and protons released by electrochemically active bacteria (EAB) in the anodic biofilm can transfer to the cathode to form H_2 with the cathodic catalyst.[4,5] The H_2 energy harvested in the MEC can be 2–4 times the input electrical energy.[1,3] However, a notable challenge in the single-chamber MEC is the H_2 sink during long term operation, mainly attributable to the H_2 scavenging by undesirable methanogenesis process.[6–8] For example, the hydrogenotrophic methanogenesis can consume 4 mol H_2 (combustion heat of 285 kJ mol^{-1}) to produce 1 mol CH_4 (combustion heat of 890 kJ mol^{-1}), resulting in significant decrease of H_2 and energy recovery.[6,9]

To inhibit the methanogenesis process in the single-chamber MEC, different strategies have been developed in recent years.[6,9,10] Chemical agents, such as 2-bromomethane sulfonate (2-BES),[4] chloroform,[11] and acetylene,[5] have been tested for the methanogen inhibitors in the MEC. With addition of 286 μM 2-bromoethanesulfonate in the MEC, methanogenic electron loss decreased from 36% to 2.5% and the overall H_2 recovery increased from 56% to 80%.[4] With the chloroform dosage of 5‰, the methane (CH_4) production was efficiently inhibited within 11 batch cycles.[11] However, the chemical inhibitors above were toxic and not sustainable during long-term operation in the MEC.[2,6] The negative pressure (40.5 kPa) control in the single-chamber MEC improved H_2 production rate and electrical energy recovery due to the inhibition of methanogen growth. However, CH_4 production became dominant in the biogas production once the negative pressure was removed.[10] It was shown that continuous H_2 extraction *via* a gas-permeable hydrophobic membrane in the MEC (*i.e.*, dual-chamber MEC) could eliminate the CH_4 production.[12] Some conditions, such as ultraviolet irradiation and low temperature, can be applied to effectively inhibit the methanogenesis in the single-chamber MEC during long-term operation. Nevertheless, applications of such conditions require high operation costs.[4,9,13] Therefore, it is necessary to develop efficient methods for methanogenesis inhibition in the single-chamber MEC.

Guangdong Provincial Key Laboratory of Environmental Pollution Control and Remediation Technology, School of Environmental Science and Engineering, Sun Yat-sen University, Guangzhou, 510006, China. E-mail: luyaobin@mail.sysu.edu.cn

Since most of methanogens prefer neutral pH conditions, pH control in the MEC has been tested to enhance H_2 production in recent years. At pH = 5.8, the CH_4 production was suppressed in the single-chamber MEC within the first two batches but recovered in the following batches, indicating that acidic pH control was not sustainable to the methanogenesis inhibition.[14,15] At pH = 9.3, H_2 production rate in the single-chamber MEC increased by 117% compared with that under the neutral condition.[16,17] The dominant species of bacterial community in anodic biofilm of the MEC are *Geoalkalibacter* sp. and *Geobacter* sp. under the alkaline and neutral conditions, respectively.[16,18,19] However, the development of methanogens in the cathodic biofilm of MEC under alkaline conditions has not been studied.

The objective of this study was to investigate H_2 production with methanogenesis inhibition in the single-chamber MEC under alkaline conditions during long-term operation. Performance of the MEC was examined at different pH values for 124 d of operation. Bacterial communities in the anodic and cathodic biofilms were analyzed and the mechanism of methanogenesis inhibition in the MEC was discussed related to H_2 production.

2. Materials and method

2.1 MEC setup and operation

Single-chamber MEC was made of glass bottle sealed with rubber stopper and epoxy resin as previously described.[9] The effective volume of each MEC was 140 mL. Graphite brush (3 cm diameter × 9 cm length) was used as the anode after heat pretreatment at 450 °C for 30 min. The cathode was made of carbon cloth (W1S1005, CeTech Co., Ltd, China) coated with 0.5 mg cm^{-2} of platinum. Effective projected surface area of the cathode was 7 cm^2. The anode and cathode were placed in the bottom and upper positions of reactor, respectively. The distance between the anode and cathode was about 4 cm.

Eight reactors were prepared during the startup stage. To avoid the light effect, the reactors were wrapped up with aluminum foil. The effluent of primary clarifier from Datan Sha Wastewater Treatment Plant, Guangzhou, China was inoculated into each reactor. The medium contained: 1 g L^{-1} CH_3COONa, 4.20 g L^{-1} $NaHCO_3$, 0.31 g L^{-1} NH_4Cl, 0.13 g L^{-1} KCl, 0.0294 g L^{-1} $K_2HPO_4 \cdot 3H_2O$, 12.5 mL L^{-1} trace metal solution and 5.0 mL L^{-1} vitamin solution, with final pH of 8.5. A 10 Ω external resistor and a power supply (IT 6720, Itech, China) were connected in series between a cathode lead and an anode lead of the MEC. The applied voltage on the MEC was controlled at 0.8 V throughout all the tests.

The reactors were refreshed when the external current in the MEC was <0.5 mA. After two batch cycles of operation, the maximum current density in the MEC was >60 A m^{-3} and the startup of MEC was over. The MEC reactors were operated for 13 cycles (~26 d) at pH of 8.5. During the 14^{th}–23^{rd} cycle (~20 d), pH in the medium was increased to 9.5 with 3.10 g L^{-1} $NaHCO_3$ and 1.38 g L^{-1} Na_2CO_3. During the 24^{th}–37^{th} cycle (~28 d), pH in the medium was increased to 10.5 with 0.80 g L^{-1} $NaHCO_3$ and 4.29 g L^{-1} Na_2CO_3. During the 38^{th}–62^{nd} cycle (~50 d), pH in the medium was increased to 11.2 with 5.30 g L^{-1} Na_2CO_3. The operation time in the MEC was controlled at ~24 h for each cycle at the different pH values. At pH = 8.5, 9.5, 10.5, and 11.2, conductivities in the anolyte were 5.2 ± 0.1, 6.0 ± 0.1, 7.5 ± 0.2, and 8.9 ± 0.2 mS cm^{-1}, respectively. All experiments were carried out at 30.0 ± 2.0 °C.

2.2 Analyses

The voltage through the external resistor was collected with a digital multimeter (model 2700, Keithley Instruments, Inc., Cleveland, OH) at every 15 min.[20,21] The anode and cathode potentials were determined *via* a saturated calomel electrode (SCE, CHI150, Chenhua Co, Shanghai, China), respectively. Chemical oxygen demand (COD) was measured using the dichromate standard method.[20,21] The pH values were measured with a pH meter (FE 20, Mettler Toledo, Swiss). The biomass on the anodic and cathodic biofilm was determined using the Coomassie brilliant blue method.[9] Biogas from the MEC was collected with sampling bags (each 0.15 L capacity, Shanghai ELOR Co., Ltd., China). The gas composition in the biogas was analyzed using gas chromatography (GC 2014, Shimadzu Co., Japan) equipped with a thermal conductivity detector.[22] The high purity argon was the carrier gas at a flow rate of 10 mL min^{-1}.[9]

2.2.1 Microbial community analysis. Anode and cathode samples were collected in the MECs at the platform of the maximum current density at pH = 8.5, 9.5, 10.5, and 11.2 in the 13^{rd}, 23^{rd}, 37^{th}, and 62^{nd} cycle, respectively. Genomic DNAs from the samples were extracted using a soil DNA kit (D5625-01, Omega Bio-Tek, USA) according to the manufacturer's manual.[22] PCR amplification was performed after 1% agarose gel electrophoresis examination on the DNA qualities. The V3–V4 regions of the bacterial 16S rRNA genes from the anode samples were amplified using the primer pairs of 338F (ACTCCTACGGGAGGCAGCA) and 806R (GGACTACVSGGGTATCTAAT).[20,21] The primers pairs of 515FmodF (GTGYCAGCMGCCGCGGTAA) and 806 RmodR (GGACTACNVGGGTWTCTAAT) were used for the amplification of the archaea and bacterial 16S rRNA genes from the cathode samples.[22] A unique 8-bp barcode was used to tag each PCR product. All the PCR amplifications were performed in 20 μL reactions, which contained 4 μL 5 × FastPfu Buffer, 2 μL dNTPs (2.5 mM), 0.8 μL forward primer (5 μM), 0.8 μL reverse primer (5 μM), 0.4 μL FastPfu polymerase, 0.2 μL bull serum albumin (BSA), 2 μL template DNA, and 9.8 μL H_2O.[22] The PCR condition for the anode samples was the same as that for the cathode samples. After being purified and quantified, the final products from PCR amplification were sequenced on an Illumina Miseq platform by Majorbio (Shanghai, China). The read sequences were joined, quality-checked, and grouped into operational taxonomic units (OTUs) at 97% similarity.[20,21] The phylum and genus levels were drawn out using the Silva database with the classified sequences. The Shannon index was calculated as previously reported.[22] Raw sequencing reads were deposited into the NCBI SRA under the project accession number SRP 202565.

2.2.2 Quantitative real-time PCR. Quantitative real-time PCR (qPCR) was used to quantify the total methanogens based on the *mcrA* genes (methanogenic archaeal methyl coenzyme-M reductase).[22,23] The qPCR analysis was conducted using Cham QSYBR Color qPCR Master Mix (Vazyme Biotech Co. Ltd., Nanjing, China) and a Real-time PCR system (ABI7300, Applied Biosystems, CA, USA). The PCR reaction procedure was as follows: 5 min of denaturation at 95 °C, 35 cycles of 30 s at 95 °C, 40 s for annealing at 55 °C, and 1 min for extension at 72 °C. Each reaction was conducted in a 20 μL solution containing 1 μL DNA template, 5 μM of each *mcrA* primer, and 10 μL reaction mix. The primer pairs were *mcrA*–f (GGTGGTGTMGGATTCACACARTAYGCWACAGC) and *mcrA*-r (TTCATTGCRTAGTTWGGRTAGTT).[23] The standard curves of qPCR assay were generated in triplicate. The standard curve parameters of qPCR containing a slope of −3.452, a *Y*-inter of 36.899, a correlation coefficient of 0.999, and an efficiency of 95%.

2.3 Calculations

The volumetric current density (I_V, A m^{-3}) was calculated based on the current normalized by the effective volume of the reactor.[9,22,24] The coulombic efficiency (CE, %) was the ratio of the total coulombs produced in the circuit of MEC to the total theoretical amount of coulombs produced based on the COD removal.[9,22,24] Hydrogen yield (mol H_2/mol acetate) was estimated according to the amount of H_2 produced by the consumed acetate.[9,22,24] Energy recovery of the MEC included electrical energy recovery (η_E, %) and total energy recovery (η_{E+S}, %).[9,22,24] The electrical energy recovery was determined by the ratio of the energy content of the produced biogases (H_2 and CH_4, based on its heat of combustion, *i.e.*, ΔH_{H_2} = 285.83 kJ mol^{-1} and ΔH_{CH_4} = 890.31 kJ mol^{-1}) to the electricity energy input.[9,22,24] The total energy recovery was calculated by the ratio of the energy content (*i.e.*, heat of combustion) of the produced biogases and the sum of the electrical energy input and the energy content of the substrate.[9,22]

3. Results

3.1 Hydrogen production in the MEC at different pH values

As shown in Fig. 1, stable and repeatable current densities were produced in the MEC at the different pH values. The maximum current density reached 64.4 ± 1.2 A m^{-3} within 13 cycles (26 d) at pH 8.5. The maximum current density increased from 68.9 ± 3.8 to 85.2 ± 1.5 A m^{-3} with pH increase from 9.5 to 10.5. At pH 11.2, the MEC was successfully operated for 25 cycles (~50 d) with the maximum current density of 83.7 ± 1.5 A m^{-3}.

The biogas composition greatly changed in the MEC within different cycles at the different pH values (Fig. 2A). At pH 8.5, the H_2 production rapidly decreased from 95 ± 2% in cycle 2 to 11 ± 5% in cycle 13. The CH_4 production increased from 0 in cycle 2 to 85 ± 5% in cycle 13. At pH 9.5, H_2 percentage was kept at 45–60% within 10 cycles (*i.e.*, 14th–23rd cycle) and CH_4 production accounted for 35–50% of the total biogas within the cycles. At pH 10.5, H_2 percentage was significantly improved to ~90%, while CH_4 percentage decreased to ~10% within 14 cycles (*i.e.*, 24th–37th cycle). At pH 11.2, H_2 and CH_4 production were kept at 85–90% and 10%, respectively, within 25 cycles (50 d), indicating that effective methanogenesis inhibition in the single-chamber MEC was realized under the alkaline condition. The CO_2 concentrations in the total biogas were almost kept at 0% throughout all the tests, mainly because of CO_2 dissolution in the alkaline solution.

Results of H_2 yields were consistent with those of the H_2 percentages in the total biogas at the different pH values (Fig. 2B). At pH 8.5, H_2 yield significantly decreased from 3.57 ± 0.20 mol H_2 per mol acetate in cycle 2 to 0.12 ± 0.10 mol H_2 per mol acetate in cycle 13. At pH 9.5, H_2 yield increased to 1.00 ± 0.20 mol H_2 per mol acetate in cycle 14 but decreased to 0.64 ± 0.12 mol H_2 per mol acetate in cycle 23. At pH 10.5, the maximum H_2 yield reached 3.21 ± 0.21 mol H_2 per mol acetate within 25 cycles and H_2 yield gradually decreased to 2.54 ± 0.23 mol H_2 per mol acetate in cycle 37. At pH 11.2, high H_2 yield was kept in a range of 2.64 ± 0.16–3.36 ± 0.10 mol H_2 per mol acetate within 50 d operation (*i.e.*, 38th–62rd cycle).

3.2 Coulombic efficiency and energy recovery in the MEC at different pH values

CE in the MEC varied from 104 ± 1% to 145 ± 5% within 62 cycles of operation (Fig. 3A). Average coulombs per cycle at pH 11.2 were slightly higher than those at pH = 8.5, 9.5, and 10.5, respectively (1242 ± 36 *vs.* 1070 ± 16, 1078 ± 17, and 1144 ± 25C). The results of CE > 100% indicated that a H_2 production-consumption loop between the anode and cathode occurred in the MEC at the different pH values.[9,25]

The energy recovery, including the electrical and overall recoveries, of the MEC is shown in Fig. 3B. At pH 8.5, the electrical recovery decreased from 146 ± 15% to 111 ± 11% within 13 cycles, which was in accordance with the change of H_2 composition in the total biogas. At pH 9.5, the electrical recovery of MEC was in a range of 124 ± 10%–133 ± 9%. At pH = 10.5 and 11.2, the maximum electrical recovery reached 202 ± 15% within 24 cycles. In the 24th–62nd cycle (~76 d), the electrical recovery gradually decreased to 154 ± 5%. Nevertheless, the average electrical recovery was higher than that at pH = 8.5 and 9.5 (171 ± 18% *vs.* 127 ± 15% and 129 ± 13%). The overall energy recovery reached 44 ± 1%–81 ± 4% within 62 cycles. The average overall energy recovery at pH 8.5 was almost the same as that at pH 9.5 (52% *vs.* 53%). The average overall energy recovery at pH = 10.5 and 11.2 reached 75 ± 5% and 72 ± 3%, respectively.

As shown in Fig. 4, the anode and cathode potentials were stable within 24 h at the different pH values. The anode potential (*vs.* SCE) at pH 8.5 was higher than those at pH = 9.5, 10.5, and 11.2, respectively (−0.122 *vs.* −0.186, −0.224, and −0.228 mV) (Fig. 4A). The cathode potentials (*vs.* SCE) were in the following order: −0.837 mV (pH 8.5) > −0.875 mV (pH 9.5) > −0.900 mV (pH 10.5) > −0.917 mV (pH 11.2) (Fig. 4B).

3.3 Microbial community analysis in the MEC at different pH values

At the phylum level, Proteobacteria, Firmicutes, and Actinobacteria dominated the microbial community in the anodic biofilm at the

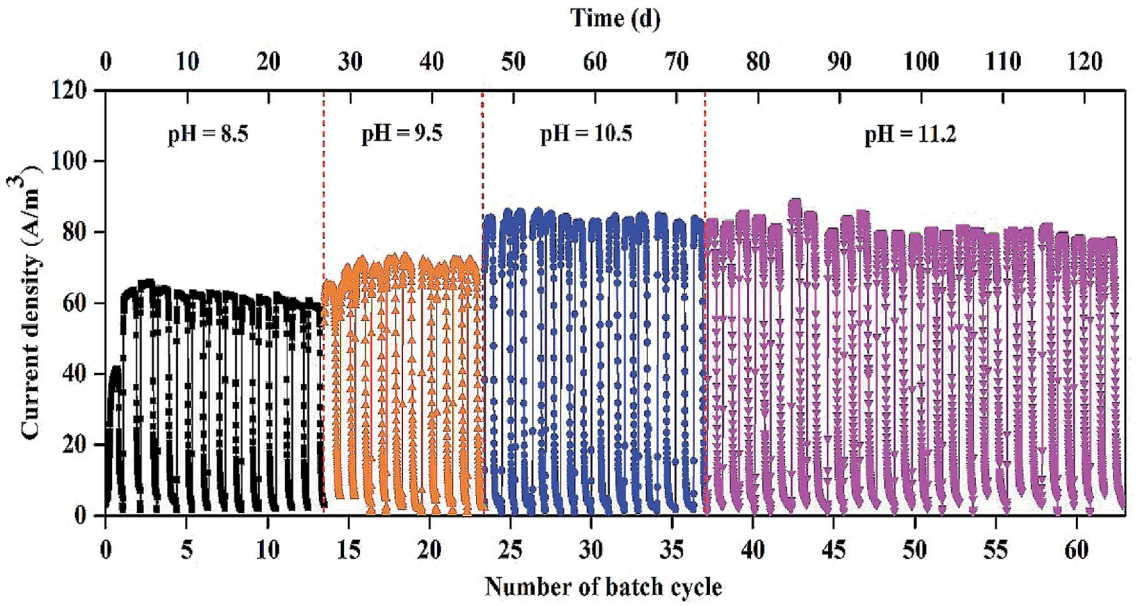

Fig. 1 Electricity generation in the single-chamber MEC at different pH conditions.

different pH values (Fig. 5A). The sum of relative abundance of Proteobacteria, Firmicutes, and Actinobacteria reached 92%, 85%, 78%, and 72% at pH = 8.5, 9.5, 10.5, and 11.2, respectively. With pH increase from 8.5 to 11.2, the relative abundance of Proteobacteria decreased from 76% to 23%, while the relative abundance of Firmicutes increased from 7.8% to 49%. At the genus level, the composition of bacterial community in the anode biofilm greatly changed with the different pH values (Fig. 5B). At pH 8.5, *Geoalkalibacter* dominated the bacterial community with the relative abundance of 73%. At pH 9.5, the relative abundance of *Geoalkalibacter* decreased to 0.31%, while the relative abundance of *Corynebacterium* increased from 7.9% at pH 8.5 to 20%. *Azoarcus* reached the highest relative abundance of 28% compared with <1.0% at pH = 8.5, 10.5, and 11.2. At pH 10.5, the relative abundance of *Geoalkalibacter* was 69%, while the relative abundance of *Corynebacterium* decreased to 0.1%. At pH 11.2, the relative abundance of *Geoalkalibacter* and *Corynebacterium* decreased to 3.0% and 0.3%, respectively. At pH 11.2, *Alkalibacter*, Clostridiaceae, and *Enterococcus* reached the highest relative abundance of 26%, 19%, and 28%, respectively. The maximum Shannon and Simpson indices in the anode biofilm were obtained at pH = 9.5 (2.69) and 10.5 (0.51), respectively (Table 1). The result indicated that the microbial community at pH = 9.5 and 10.5 had the highest richness and evenness, respectively.[26,27]

In the cathodic biofilm, the microbial community at the different pH values was dominated by Proteobacteria and Euryarchaeota at the phylum level (Fig. 6A). The highest relative abundance of Euryarchaeota was 73% at pH 11.2 compared with 18% (pH 8.5), 70% (pH 9.5), and 17% (pH 10.5). The relative abundance of Proteobacteria decreased from 54% at pH 8.5 to 3.5% at pH 11.2. At the genus level, the microbial community in the cathodic biofilm was significantly different from that in the anodic biofilm at the different pH values (Fig. 6B). At pH 8.5, Methanobacteriaceae and *Geoalkalibacter* dominated the microbial community in the cathodic biofilm with the relative abundance of 18% and 51%, respectively. At pH 9.5, the relative abundance of Methanobacteriaceae significantly increased to 70% but *Geoalkalibacter* decreased to <1%. At pH 10.5, *Corynebacterium* reached the highest relative abundance of 20% compared with 8.8% (pH 8.5), 9.6% (pH 9.5), and 11% (pH 11.2). Methanobacteriaceae and *Geoalkalibacter* accounted for 16% and 27%, respectively. At pH 11.2, *Geoalkalibacter* and *Corynebacterium* decreased to <1.1% and 11%, respectively. Methanobacteriaceae reached the highest relative abundance of 73%. The microbial community in the cathodic biofilm at pH = 10.5 and 11.2 had the highest richness and evenness, respectively, according to the Shannon (2.80) and Simpson (0.55) indices (Table 1).

3.4 Quantitative real-time PCR on methanogens in the cathodic biofilm

The number of total methanogens in the cathodic biofilm decreased with the increase of pH according to the qPCR results (Table 1). The gene copy number of methanogens at pH 11.2 was 34% of that at pH 8.5 (2.23 ± 0.46 *vs.* $6.52 \pm 0.60 \times 10^8$ copy per cm^2). The results of gene copy number of methanogens were in accordance with those of cathodic biomass (Table 1). The cathodic biomass at pH 11.2 was only 16.6% of that at pH 8.5 (0.02 ± 0.00 *vs.* 0.12 ± 0.01 mg protein per g). Correspondingly, the anodic biomass decreased by 33% with pH increase from 8.5 to 11.2 (0.61 ± 0.05 *vs.* 0.41 ± 0.11 mg protein per g). The results indicated that higher alkaline condition significantly inhibited Archaea and bacteria growth on the cathode.

4. Discussion

The performance for H_2 production of our MEC at pH 11.2 was comparable to that of other MECs with different strategies of

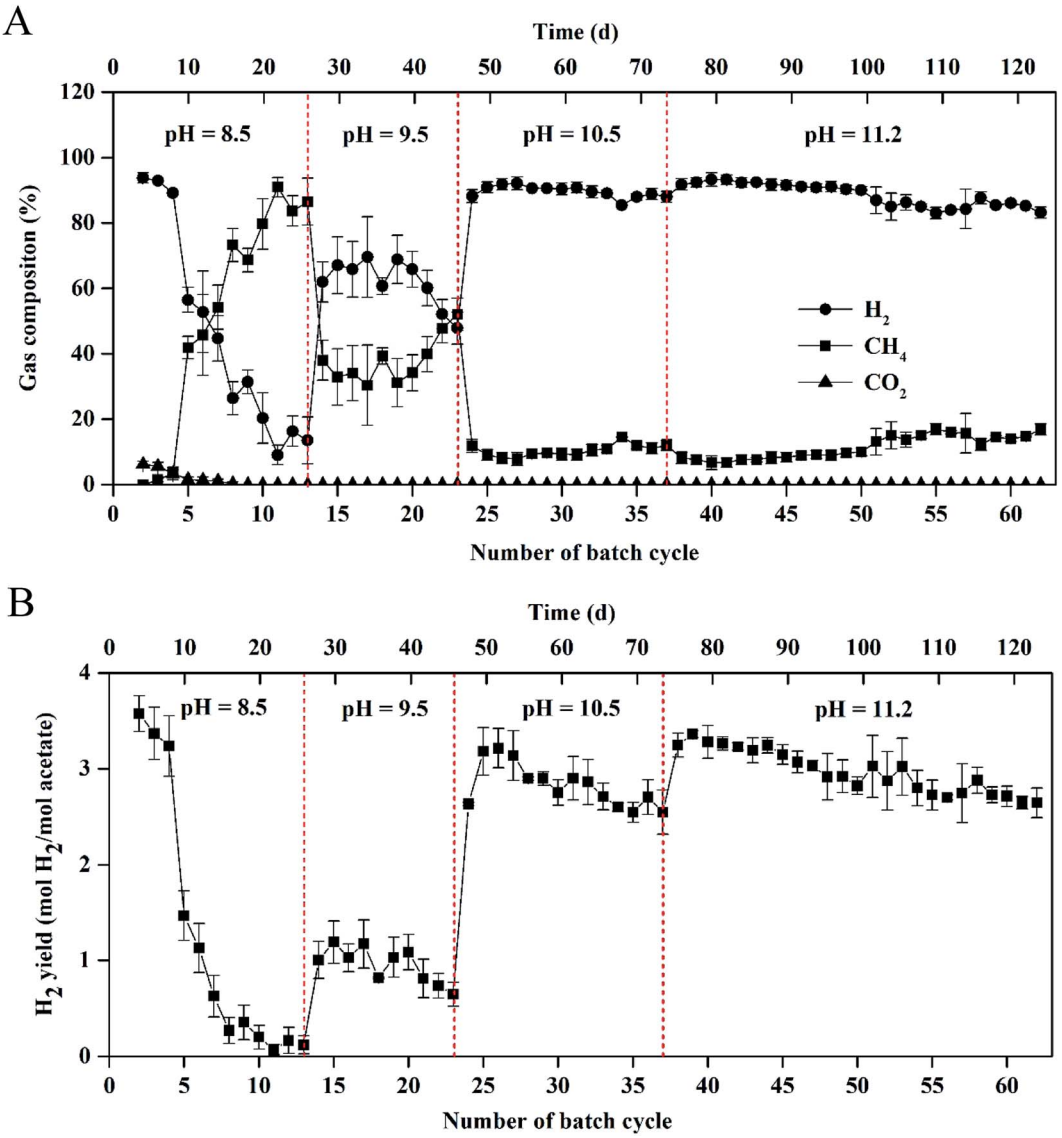

Fig. 2 (A) Gas composition and (B) hydrogen yield in the single-chamber MEC at different pH conditions.

methanogenesis inhibition. The H_2 production in our MEC at pH 11.2 was much higher than that with addition of 1% acetylene and 5 mM 2-bromoethanesulfonate inhibitors, respectively (85–90% *vs.* 60–70%).[5] The H_2 yield in our MEC was comparable to that in the MEC with UV irradiation (2.64–3.36 *vs.* 2.87–3.70 mol H_2 per mol acetate).[9] The current density in our MEC at pH 11.2 was higher than that at pH = 9.3 (83.7 *vs.* ~2 A m^{-3}).[16] Moreover, many strategies (*e.g.*, UV irradiation, chemical agents, and negative pressure control) could not inhibit CH_4 production effectively once methanogenesis was well established in the MEC.[6,9,10] Our alkaline adjustment with pH 11.2 could significantly improve H_2 production even after produced CH_4 dominated the whole biogas in the MEC. Therefore, the alkaline adjustment should be an effective method for methanogenesis inhibition in the single-chamber MEC.

The better performance of our MEC at pH 11.2 was attributed to low cathodic biomass (0.02 ± 0.00 mg protein per g), low abundance of methanogens in the cathodic biofilm (2.23 ± 0.46 × 10^8 copy per cm^2), and low anode potential (−0.228 mV *vs.* SCE). The low abundance of methanogens in the cathodic biofilm resulted in less CH_4 production in the single-chamber MEC.[9,28] The low cathodic biomass resulted in less acetate consumption in the cathode, and enhanced acetate utilization by EABs on the anode.[9] The low anode potential was beneficial to improve the activity of EABs on the anodic biofilm.[29]

Many bacteria and Archaea identified in our single-chamber MEC have been reported in various bioelectrochemical systems (BESs). In the cathodic biofilm of BESs, Methanobacteriaceae has been widely identified as a dominated hydrogenotrophic methanogen.[22] The relative abundance of Methanobacteriaceae in the microbial community reached 77.2% in the thickness of 45–60 μm within the cathodic biofilm in the single chamber MEC.[22] The copy number of *mcrA* gene within the cathodic biofilm in the MEC greatly varied because of different

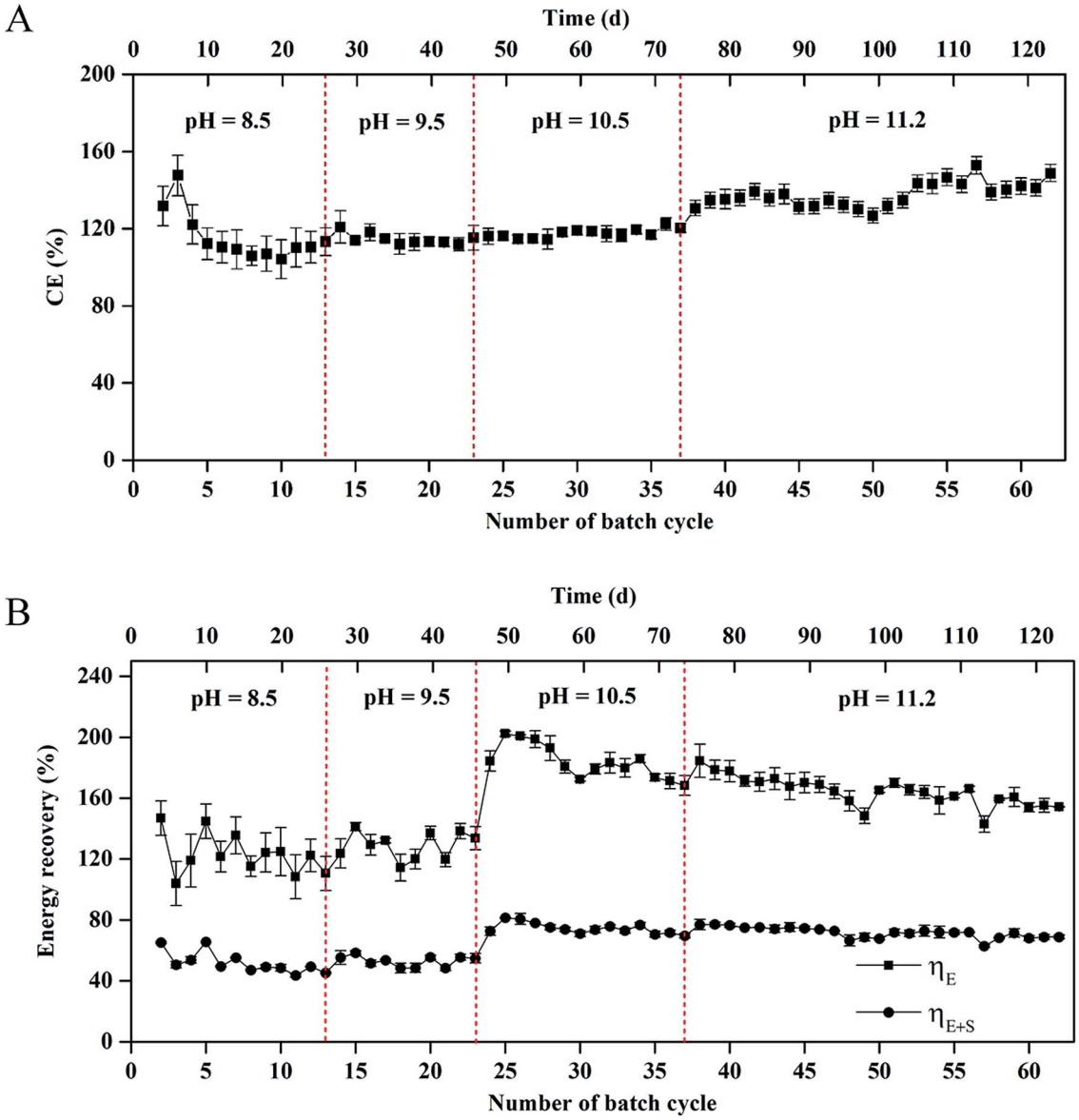

Fig. 3 (A) Coulombic efficiency and (B) energy recovery in the single-chamber MEC at different pH conditions.

substrates, inoculums, and operation conditions.[30–33] The *mcrA* gene copy number in the cathodic biofilm of our MEC was similar to that of the mini-MEC with the inoculums of anaerobic digestion sludge at pH 7.0 ($\sim 10^8$ copy per cm^2).[30] The relative abundance of Methanobacteriaceae was not equivalent to the absolute quantity of Methanobacteriaceae in the microbial community. At pH 11.2, Methanobacteriaceae reached high relative abundance of 73%, but low absolute quantity (*i.e.*, *mcrA* gene copy number). The growth of Methanobacteriaceae was greatly inhibited with significant decrease of the *mcrA* gene copy number and cathodic biomass. The low amount of Methanobacteriaceae resulted in low CH_4 production and high H_2 production. The change of Methanobacteriaceae was consistent with the performance of our MEC under the alkaline condition. Although *Geoalkalibacter* and *Corynebacterium* have seldom been found in the cathodic biofilm of MEC under alkaline conditions so far, other EABs (*e.g.*, *Geobacter* and Desulfobacteraceae) have been identified in the cathodic biofilm under the neutral condition.[23,32,34] The relative abundance of *Geobacter* could reach 30–45% within the bacterial community in the cathodic biofilm.[32] The synergistic effect among *Geoalkalibacter*, *Corynebacterium*, and Archaea within the cathodic biofilm on H_2 production is unclear, which needs to be further explored. Homoacetogens have been frequently identified in the MEC fed with acetate, which can utilize H_2 and produce acetate to form an internal H_2 cycle in the MEC.[35] High presence of homoacetogens may greatly decrease the efficiency of H_2 production and result in CE as high as 1242%.[35] However, homoacetogens (*e.g.*, *Acetobacterium*) were not identified in the microbial communities in this study. Efficient inhibition of homoacetogen growth should be helpful for increasing H_2 production,[35] attributable to better performance of our MEC compared to other MECs with different strategies of methanogenesis inhibition.

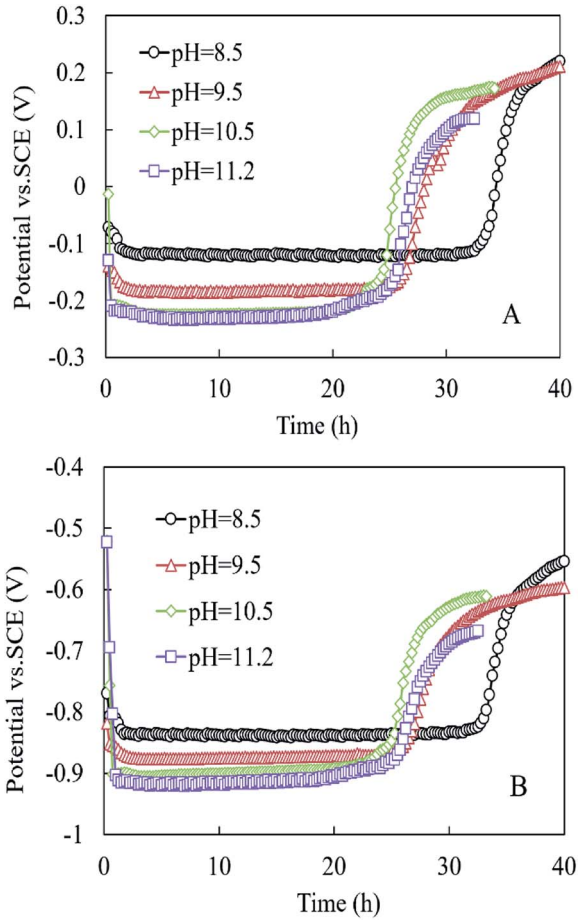

Fig. 4 (A) Anode potential and (B) cathode potential in the MEC within one cycle at different pH conditions.

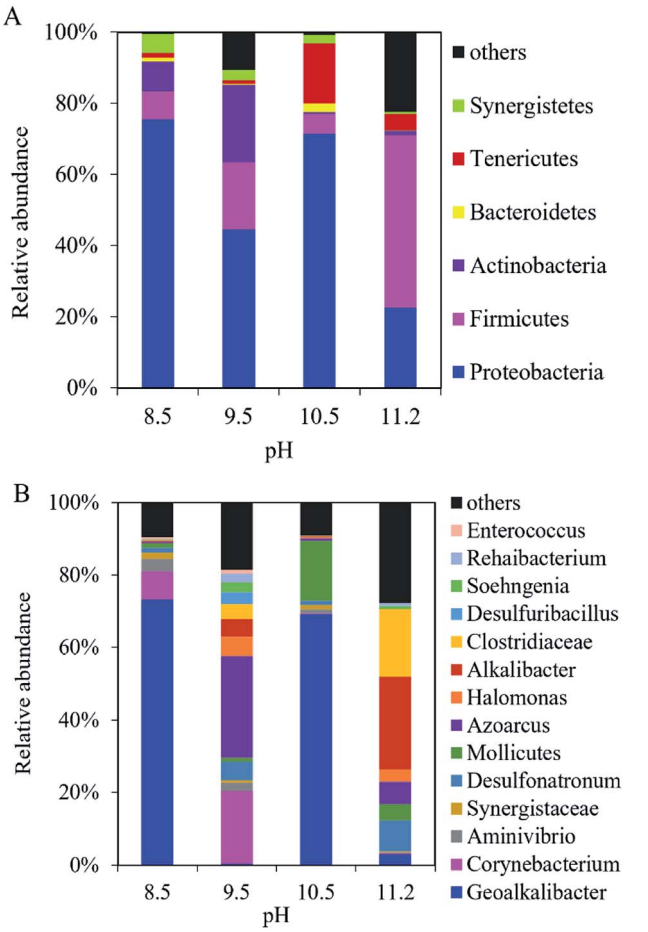

Fig. 5 Composition of bacteria community in the anodic biofilm of the single-chamber MEC at different pH conditions at (A) the phylum level and (B) the genus level.

In the anodic biofilm of BESs, *Geoalkalibacter* has been identified as an EAB with high electricity generation.[16,18] The relative abundance of *Geoalkalibacter* reached 43% and 9.8% in the bacterial community of the anodic biofilm in the MEC fed with acetate and glycerol at pH 9.3, respectively.[16,17] The relative abundance of *Geoalkalibacter* greatly changed at pH = 8.5–11.2 in this study, indicating that the growth of EABs in the anode biofilm was sensitive to pH in the solution. The total biomass in the anode significantly decreased with pH from 8.5 to 11.2. Therefore, it is necessary to determine the optimal pH for *Geoalkalibacter* growth using pure *Geoalkalibacter* strain in the future. In addition, *Corynebacterium* (*e.g.*, *Corynebacterium* sp. strain MFC03) was capable of generating electricity in a pH range of 8.0–10.0.[36] The optimal pH for *Corynebacterium* sp. strain MFC03 to produce electricity was 9.0.[37] *Corynebacterium* was detected with the relative abundance of 32.8% in the bacterial community in the anodic biofilm of MFC fed with glucose and *p*-nitrophenol at pH = 7.0.[31] As a strictly anaerobic and an alkaliphilic bacterium, *Alkalibacter* has been identified in the alkaline MFC and MEC.[16] Therefore, *Geoalkalibacter* and *Corynebacterium* identified in this study might have high activity under alkaline condition. Moreover, the protons released by exoelectrogens (*e.g. Geoalkalibacter* and *Corynebacterium*) can significantly decrease the pH in solution close to the anode biofilm, resulting in high alkaline endurance of EABs.

The carbonate buffer used in this study is also useful for accelerating the proton transfer from anode to cathode and improving the reaction activity of the anode and cathode (*e.g.*, potential) in the MEC. To the anode, acetate can be degraded by EABs with to produce electrons and protons as follows:[38,39]

$$\text{Anode}: CH_3COO^- + 4H_2O \xrightarrow{\text{exoelectrogens}} 2HCO_3^- + 9H^+ + 8e^- \quad (1)$$

In the electrolyte with carbonate buffer solution, excess H^+ can be neutralized by OH^- from the CO_3^{2-} hydrolysis as follows:

$$H^+ + OH^- \rightarrow H_2O \quad (2)$$

$$CO_3^{2-} + H_2O \rightarrow HCO_3^- + OH^- \quad (3)$$

To the cathode, HCO_3^- can release H^+ on the cathode to produce H_2:[38]

$$HCO_3^- \rightarrow CO_3^{2-} + H^+ \quad (4)$$

Table 1 Characteristics of the microbial communities and biomasses in the anodic and cathodic biofilms of the single-chamber MEC

Biofilm	pH	Shannon index	Simpson index	Biomass (mg protein per g)	*mcrA* gene copy number ($\times 10^8$ copy per cm^2)
Anode	8.5	1.37	0.54	0.61 ± 0.05	—
	9.5	2.69	0.13	0.65 ± 0.06	—
	10.5	1.30	0.51	0.44 ± 0.04	—
	11.2	2.34	0.15	0.41 ± 0.11	—
Cathode	8.5	1.91	0.30	0.12 ± 0.01	6.52 ± 0.60
	9.5	1.53	0.50	0.07 ± 0.01	6.18 ± 0.24
	10.5	2.80	0.14	0.02 ± 0.00	4.60 ± 0.18
	11.2	1.26	0.55	0.02 ± 0.00	2.23 ± 0.46

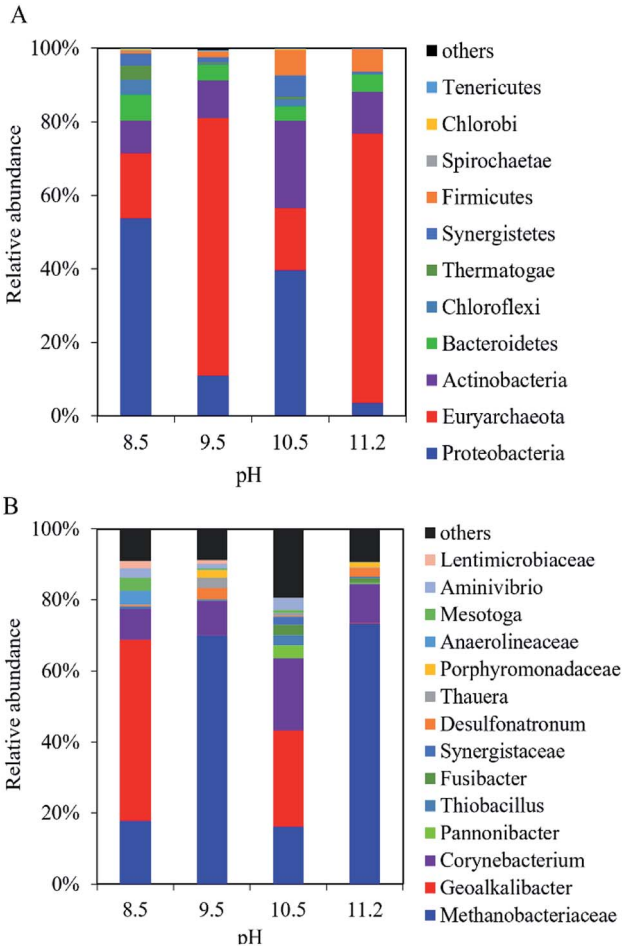

Fig. 6 Composition of microbial community in the cathodic biofilm of the single-chamber MEC at different pH conditions at (A) the phylum level and (B) the genus level.

$$2H^+ + 2e^- \xrightarrow{\text{Catalyst}} 2H_2 \quad (5)$$

Therefore, bicarbonate (HCO_3^-) plays an important role as pH buffer and proton carrier under an alkaline condition.[38] With indirect transportation of H^+, our MEC could produce hydrogen efficiently. Moreover, high electron transfer ability under high pH was helpful for high H_2 production. According to the Nernst equation, the anode and cathode equilibrium potentials can be calculated as follows:[40]

$$E_{an} = E_{an}{}^0 - \frac{RT}{8F}\ln\frac{[CH_3COO^-]}{[HCO_3^-]^2[H_{an}^+]^9} \quad (6)$$

$$E_{cat} = E_{cat}{}^0 - \frac{RT}{2F}\ln\frac{pH_2}{[H_{cat}^+]^2} \quad (7)$$

Here E_{an} and E_{cat} are the equilibrium anode and cathode potentials, respectively; $E_{an}{}^0$ and $E_{cat}{}^0$ are the standard anode and cathode potentials, respectively; $[CH_3COO^-]$ and $[HCO_3^-]$ are the concentrations of acetate and bicarbonate in the solution, respectively; $[H_{an}^+]$ and $[H_{cat}^+]$ are the concentrations of protons in the anode and cathode, respectively; pH_2 represents the H_2 concentration;[40] R and F are constants; and T is the temperature (K). With pH increase from 8.5 to 11.2, the concentrations of HCO_3^- decreased in the solution, resulting in increase of the $\frac{RT}{8F}\ln\frac{[CH_3COO^-]}{[HCO_3^-]^2[H_{an}^+]^9}$ value. Thus the equilibrium anode potential (E_{an}) decreased with pH from 8.5 to 11.2. Due to the H_2 production improvement with the pH increase from 8.5 to 11.2, the values of $\frac{RT}{2F}\ln\frac{pH_2}{[H_{cat}^+]^2}$ increased, resulted in the decrease of the equilibrium cathode potential (E_{cat}). The results of the theoretical potential analysis were consistent with the measurements on the anode and cathode potentials in this study. And the activity of EABs on the anodic biofilm can be improved by the low anode potential.

Our results demonstrate for the first time the operation of MEC at pH 11.2. Various EABs such as *Geoalkalibacter* and *Corynebacterium* in the anodic biofilm at pH 11.2 suggest that the extracellular electron transfer to anode may be independent of the optimal pH for the growth of EABs. High current density in the MEC at pH 11.2 indicated that the extracellular electron transfer rate under alkaline condition may be faster than that under neutral condition. It should be interesting to explore the extracellular electron transfer mechanism among mixed EABs under alkaline condition. Moreover, the configuration and position of the anode and cathode in the scale-up MEC should be optimized to enhance the bubble formation and accelerate the release dynamics of H_2. Alkaline wastewater discharged from

various industries may contain many organics.[41,42] For example, the pH value in yogurt wastewater can be > 11.0.[41] Such alkaline industrial wastewater may be used for H_2 production in the MEC.

5. Conclusions

It was the first time to report the excellent performance for H_2 production of single-chamber MEC at pH 11.2 with effective methanogenesis inhibition within 50 d operation. The maximum current density reached 83.7 ± 1.5 A m^{-3} with the electrical recovery of 171 ± 18% and overall energy recovery of 44–81%. At pH 11.2, H_2 production was kept at 85–90% and CH_4 production was <15% within 25 cycles (50 d). The good performance of the MEC at pH 11.2 was attributable to low abundance of methanogens within the cathodic biofilm, low cathodic biomass, and low anode potential.

Conflicts of interest

There are no conflicts to declare.

Acknowledgements

This work was partially supported by grants from the National Natural Science Foundation of China (No. 51608547, 51308557 and 51278500), the National Key R&D Program of China (No. 2017YFB0903700 and 2017YFB0903703), the program of Guangdong Science & Technology Department (No. 2017A010104007).

References

1 H. Liu, S. Grot and B. E. Logan, *Environ. Sci. Technol.*, 2005, **39**, 4317–4320.
2 L. Lu and Z. J. Ren, *Bioresour. Technol.*, 2016, **215**, 254–264.
3 S. Cheng and B. E. Logan, *Proc. Natl. Acad. Sci. U. S. A.*, 2007, **104**, 18871–18873.
4 K.-J. Chae, M.-J. Choi, K.-Y. Kim, F. F. Ajayi, I.-S. Chang and I. S. Kim, *Int. J. Hydrogen Energy*, 2010, **35**, 13379–13386.
5 L. Wang, S. Trujillo and H. Liu, *Bioresour. Technol.*, 2019, **274**, 557–560.
6 A. Kadier, M. S. Kalil, K. Chandrasekhar, G. Mohanakrishna, G. D. Saratale, R. G. Saratale, G. Kumar, A. Pugazhendhi and P. Sivagurunathan, *Bioelectrochemistry*, 2018, **119**, 211–219.
7 A. Ding, Y. Yang, G. Sun and D. Wu, *Chem. Eng. J.*, 2016, **283**, 260–265.
8 M. Sugnaux, M. Happe, C. P. Cachelin, A. Gasperini, M. Blatter and F. Fischer, *Chem. Eng. J.*, 2017, **324**, 228–236.
9 Y. Hou, H. Luo, G. Liu, R. Zhang, J. Li and S. Fu, *Environ. Sci. Technol.*, 2014, **48**, 10482–10488.
10 H. Feng, L. Huang, M. Wang, Y. Xu, D. Shen, N. Li, T. Chen and K. Guo, *Int. J. Hydrogen Energy*, 2018, **43**, 17556–17561.
11 J. Zhang, Y. Bai, Y. Fan and H. Hou, *J. Biosci. Bioeng.*, 2016, **122**, 488–493.
12 L. Lu, D. Hou, X. Wang, D. Jassby and Z. J. Ren, *Environ. Sci. Technol. Lett.*, 2016, **3**, 286–290.
13 L. Lu, N. Ren, X. Zhao, H. Wang, D. Wu and D. Xing, *Energy Environ. Sci.*, 2011, **4**, 1329–1336.
14 H. Hu, Y. Fan and H. Liu, *Water Res.*, 2008, **42**, 4172–4178.
15 S. Yossan, L. Xiao, P. Prasertsan and Z. He, *Int. J. Hydrogen Energy*, 2013, **38**, 9619–9624.
16 L. Rago, J. A. Baeza and A. Guisasola, *Bioelectrochemistry*, 2016, **109**, 57–62.
17 M. Badia-Fabregat, L. Rago, J. A. Baeza and A. Guisasola, *Int. J. Hydrogen Energy*, 2019, **44**, 17204–17213.
18 J. P. Badalamenti, R. Krajmalnik-Brown and C. I. Torres, *mBio*, 2013, **4**, e00144-13.
19 C. Lin, P. Wu, Y. Liu, J. W. C. Wong, X. Yong, X. Wu, X. Xie, H. Jia and J. Zhou, *Chem. Eng. J.*, 2019, **365**, 1–9.
20 B. Ye, H. Luo, Y. Lu, G. Liu, R. Zhang and X. Li, *Bioresour. Technol.*, 2017, **244**, 913–919.
21 G. Liu, Y. Zhou, H. Luo, X. Cheng, R. Zhang and W. Teng, *Bioresour. Technol.*, 2015, **198**, 87–93.
22 X. Li, C. Zeng, Y. Lu, G. Liu, H. Luo and R. Zhang, *Bioresour. Technol.*, 2019, **274**, 403–409.
23 W. Cai, W. Liu, Z. Zhang, K. Feng, G. Ren, C. Pu, H. Sun, J. Li, Y. Deng and A. Wang, *Water Res.*, 2018, **136**, 192–199.
24 D. Call and B. E. Logan, *Environ. Sci. Technol.*, 2008, **42**, 3401–3406.
25 G. K. Rader and B. E. Logan, *Int. J. Hydrogen Energy*, 2010, **35**, 8848–8854.
26 K. L. Lesnik and H. Liu, *Appl. Microbiol. Biotechnol.*, 2014, **98**, 4187–4196.
27 J. F. Wang, X. S. Song, Y. H. Wang, B. Abayneh, Y. H. Li, D. H. Yan and J. H. Bai, *Bioresour. Technol.*, 2016, **221**, 358–365.
28 L. Wang, L. Singh and H. Liu, *Int. J. Hydrogen Energy*, 2018, **43**, 13064–13071.
29 R. C. Wagner, D. I. Call and B. E. Logan, *Environ. Sci. Technol.*, 2010, **44**, 6036–6041.
30 M. Siegert, X.-F. Li, M. D. Yates and B. E. Logan, *Front. Microbiol.*, 2015, **5**, 778.
31 M. Cerrillo, M. Viñas and A. Bonmatí, *Renewable Energy*, 2018, **120**, 178–189.
32 M. Siegert, M. D. Yates, A. M. Spormann and B. E. Logan, *ACS Sustainable Chem. Eng.*, 2015, **3**, 1668–1676.
33 H. Rismani-Yazdi, S. M. Carver, A. D. Christy, Z. Yu, K. Bibby, J. Peccia and O. H. Tuovinen, *Bioresour. Technol.*, 2013, **129**, 281–288.
34 M. Cerrillo, M. Vinas and A. Bonmati, *ACS Sustainable Chem. Eng.*, 2017, **5**, 8852–8859.
35 L. Rago, Y. Ruiz, J. A. Baeza, A. Guisasola and P. Cortés, *Bioelectrochemistry*, 2015, **106**, 359–368.
36 M. Liu, Y. Yuan, L. X. Zhang, L. Zhuang, S. G. Zhou and J. R. Ni, *Bioresour. Technol.*, 2010, **101**, 1807–1811.
37 H. Zhao and C.-H. Kong, *Chem. Eng. J.*, 2018, **339**, 424–431.
38 Y. Fan, H. Hu and H. Liu, *Environ. Sci. Technol.*, 2007, **41**, 8154–8158.
39 R. C. Tice and Y. Kim, *Int. J. Hydrogen Energy*, 2014, **39**, 3079–3086.
40 M. Villano, C. Ralo, M. Zeppilli, F. Aulenta and M. Majone, *Bioelectrochemistry*, 2016, **107**, 1–6.
41 H. Luo, G. Xu, Y. Lu, G. Liu, R. Zhang, X. Li, X. Zheng and M. Yu, *RSC Adv.*, 2017, **7**, 32826–32832.
42 M. Prisciandaro, G. M. di Celso and F. Veglio, *Water Res.*, 2005, **39**, 5055–5063.